Sensors and Materials, Vol. 35, No. 6 (2023) 1823–1834
MYU Tokyo

S & M 3291

Effects of La^{3+} Ion Doping Concentration on the Crystal Structure and Photoluminescence Properties of $Y_{0.998}Pr_{0.002}InGe_2O_7$ Single-phased White Light-emitting Phosphor

Lay-Gaik Teoh,[1] Sean Wu,[2] Hao-Long Chen,[1] Kuan-Ting Liu,[3] and Yee-Shin Chang[4*]

[1]Department of Mechanical Engineering, National Pingtung University of Science and Technology, Neipu, Pingtung 912, Taiwan
[2]Department of Chemical and Material Engineering & Master's, Lunghwa University of Science and Technology, Guishan, Taoyuan 333, Taiwan
[3]Department of Electronic Engineering, Cheng Shiu University, Kaohsiung 347, Taiwan
[4]Department of Electronic Engineering, National Formosa University, Huwei, Yunlin 632, Taiwan

(Received January 7, 2023; accepted May 2, 2023)

Keywords: strain sensor, Pr^{3+} ion, single-phased white light-emitting phosphor

The raw materials of La^{3+} ion-doped $Y_{0.998}Pr_{0.002}InGe_2O_7$ phosphor were mixed by a vibration mill method, then calcined at 1200 °C for 10 h in air by a solid-state reaction. Regardless of the La^{3+} ion doping concentration, the La^{3+} ion did not change the crystal structure, but the luminescence properties including both the excitation and emission intensities did change. The saturation emission intensity excited by a deep UV light for the phosphor increased when the La^{3+} ion doping content was 10 mol%. As the La^{3+} ion with a large radius was introduced as a substitute for the Y^{3+} ion with a small radius in the $Y_{0.998}Pr_{0.002}InGe_2O_7$ system, an increase in compressive strain led to a decrease in oxygen vacancy concentration, which changed the emission intensity of $^1D_2 \rightarrow {}^3H_4$ and $^3P_0 \rightarrow {}^3H_4$ radiations for Pr^{3+} ion 4f–4f transition. The Commission Internationale de L'Eclairag (CIE) color coordinates of the La^{3+} ion-doped $Y_{0.998}Pr_{0.002}InGe_2O_7$ phosphor shifted slightly, but all were in the white light region at various La^{3+} ion doping contents. This provides an intelligent method for improving the luminescence properties of $Y_{0.998}P_{r0.002}InGe_2O_7$ single-phased white light-emitting phosphors for white LEDs. In addition, various emission intensity ratios of the $^1D_2 \rightarrow {}^3H_4$ and $^3P_0 \rightarrow {}^3H_4$ radiations enable the phosphors to be applied to oxygen gas sensors.

1. Introduction

White light-emitting diodes (WLEDs) are popular candidates for future green lighting systems. They use a blue LED (450–470 nm) to excite yellow phosphors (YAG:Ce^{3+} and TAG:Ce^{3+}) in commercial optical devices.[1,2] Among these commercial phosphors, much attention had been given to oxide-based phosphors for screen applications such as in plasma display panels, field emission displays, and WLEDs, because the chemical stability of oxide-based phosphors is higher than that of sulfide-based phosphors.[3,4] Nevertheless, some

*Corresponding author: e-mail: yeeshin@nfu.edu.tw
https://doi.org/10.18494/SAM4304

ISSN 0914-4935
https://myukk.org/

drawbacks of commercial optical devices were found. For example, these phosphors have poor Commission Internationale de L'Eclairag (CIE) color coordinates, which result in a low color rendering index because they are deficient in the red-emitting component.[1,2] To obtain high color purity, emission intensity, quantum efficiency, and so on, many efforts had been made; for instance, oxide-based phosphors were produced for solid-state lighting applications.

In general, crystal defects are formed during the synthesis of oxides at high temperatures. The point defect of oxygen vacancy often affects the optical properties of phosphors. It was shown that the effective energy transfer from host to activator ions is by way of oxygen vacancies, and appropriate concentrations of oxygen vacancies could be a sensitizer to enhance the photoluminescence (PL) properties of phosphors.[5] If the oxygen vacancy concentration is very high, the electrons trapped by temperature control in particular oxygen vacancy sites will be gradually released, and this causes a long delay in light emission during the actual PL process.

Many studies have shown that decreasing the oxygen vacancy concentration will contribute to the enhancement of the PL properties of phosphors, which can be performed by adding fluxes,[6] using the wet chemical method to reduce the calcination temperature,[7,8] or by doping with ions with different radii to decrease the distortion degree of the lattice symmetry.[9] Among these methods, doping with ions with different radii is the most effective. For example, when a Ca^{2+} ion is replaced by a Sr^{2+} ion in the $Ca_2La_{0.97}Pr_{0.03}TaO_6$ host, the lattice becomes distorted, and an increased compressive strain is induced around the Pr^{3+} ions. This causes the emission intensity of Sr^{3+} ion-doped phosphors to be greater than that of Sr^{2+} ion-free phosphors.[9]

According to our previous study,[10] $YInGe_2O_7$:xPr^{3+} phosphors can be obtained by a solid-state reaction. Under 263 nm wavelength excitation, the best condition for the white light emission of the Pr^{3+} ion-doped $YInGe_2O_7$ phosphor is obtained when the Pr^{3+} ion content is 0.2 mol%. A phosphor with single-phased white light emission properties has a great potential for white LED applications, and the luminescence properties can be improved by synthetic techniques and selecting new host materials. In this study, in order to increase the luminescence efficiencies of phosphors, various contents of La^{3+} ion-doped $Y_{0.998}Pr_{0.002}InGe_2O_7$ phosphor synthesized using a solid-state reaction were used to decrease the oxygen vacancy concentration by increasing the compressive strain around the Pr^{3+} ion center.

Furthermore, some research results showed that a Pr^{3+} ion-doped oxide material has superior PL properties, and this can be used in optical gas sensors.[11] Compared with electrical gas sensors, optical gas sensors have some advantages such as remote operation ability and applicability in the presence of electromagnetic radiation. For Pr^{3+} ion-based phosphor, it has been revealed that the emission peak intensity ratio of the $^1D_2 \rightarrow {}^3H_4$ transition to the $^3P_0 \rightarrow {}^3H_4$ transition of the Pr^{3+} ion determines the response to oxygen absorption at room temperature. It can be explained that a decrease in the energy position of the intervalence charge transfer state (IVCTS) (between $^3P_0$ and $^1D_2$) is induced to enhance the $^1D_2 \rightarrow {}^3H_4$ radiation and decrease the $^3P_0 \rightarrow {}^3H_4$ radiation when the oxygen content increases, and to give an obvious response to oxygen gas sensing.[11,12] In this study, the effects of La^{3+} ion doping on the resulting crystal structure, strain, and luminescence properties of the $(Y_{0.998-x}La_x)Pr_{0.002}InGe_2O_7$ phosphor were also examined.

2. Materials and Methods

Phosphors for $YInGe_2O_7$ doped with various Pr^{3+} ion contents were synthesized by the vibration mill method and then by a solid-state reaction at 1200 ℃ for 10 h in air. The initial materials used were Y_2O_3, In_2O_3, GeO_2, and Pr_2O_3 powders; all of them have 99.99% purity and were purchased from Aldrich Chemical Company. Initially, they were ground with zirconia balls in a polyethylene jar by a high-energy vibration-milled method for 15 min. After grinding, the mixtures were placed in an alumina crucible, then calcined at 1250 ℃ for 12 h in a programmable furnace.

To identify the phases formed after calcination, the structure of the synthesized phosphors was analyzed by X-ray powder diffraction (XRD, Bruker AXS GmbH, D8 Advance, Germany), which uses Cu Ka radiation with a source power of 30 kV and a current of 20 mA. The Hitachi U-3010 UV-vis spectrophotometer (Tokyo, Japan) was used to measure the optical absorption behavior of the phosphors at room temperature. A Hitachi F-7000 fluorescence spectrophotometer with a 150 W xenon arc lamp as the light source and a wavelength range from 200 to 700 nm was used to investigate both the excitation and emission characteristics of the phosphors.

3. Results and Discussion

Yttrium germanate oxide ($YInGe_2O_7$) has a thortveitite structure with a symmetry of C2/m space group belonging to the monoclinic system. The unit cell lattice parameters are a = 6.8286 Å, b = 8.8836 Å, and c = 4.9045 Å. The ions of In^{3+} and Y^{3+} occupy octahedral sites to form a hexagonal arrangement along the ab plane.[13] Figure 1 shows the XRD analysis results of various La^{3+} ion contents doped into the $Y_{0.998}Pr_{0.002}InGe_2O_7$ phosphor calcined at 1200 ℃ for

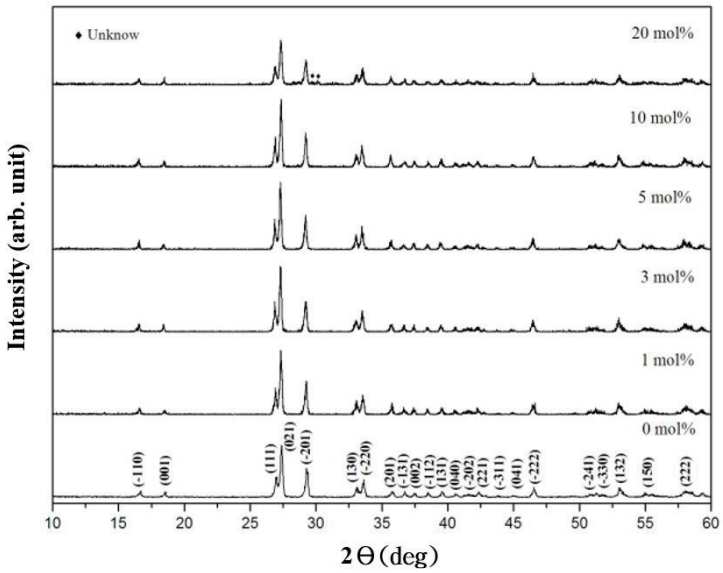

Fig. 1. XRD patterns of various La^{3+} ion contents doped into $Y_{0.998}Pr_{0.002}InGe_2O_7$ phosphor calcined at 1200 ℃ for 10 h.

10 h. The XRD patterns were the same for the $Y_{0.998}Pr_{0.002}InGe_2O_7$ phosphors doped with La^{3+} ion contents from 0 to 10 mol%, and they reveal a single phase without any impurities. This indicates that the La^{3+} ion is doped into the $Y_{0.998}Pr_{0.002}InGe_2O_7$ lattice, replacing the Y^{3+} ion to form a solid solution. For the La^{3+} ion content of 20 mol%, there are two small unknown diffraction peaks that appear near $2\theta = 30^o$, suggesting that the La^{3+} ion contents exceed the solubility limit for the $(Y_{0.998-x}La_x)Pr_{0.002}InGe_2O_7$ system.

The lattice parameters and structure of $(Y_{0.998-x}La_x)Pr_{0.002}InGe_2O_7$ (x = 0–0.2), which were determined from the X-ray diffraction profile using the *Unit Cell* computer program, are shown in Table 1. The results reveal that the compound doped with different La^{3+} ion concentrations did not show a change in crystal structure, but the lattice parameters changed when x was increased. This is because the La^{3+} ion radius (1.032 Å) is larger than the Y^{3+} ion radius (0.9 Å).

The distortion of lattice symmetry will occur and internal strain will be generated in the lattice environment when the host element is replaced by different ions with various radii. The equation proposed by Williamson and Hall can be used to calculate the internal effective strain values related to the concentrations of oxygen vacancies.[9] The equation is as follows:[14]

$$\frac{\beta\cos\theta}{\lambda} = \frac{2\eta\sin\theta}{\lambda} + \frac{1}{d}, \tag{1}$$

where β is the full width at half maximum (FWHM) in radians measured in XRD patterns, θ is the diffraction angle of the specified peak, λ is the X-ray wavelength, d is the grain size, and η is the effective strain.

Table 2 shows the η and d values of the $(Y_{0.998-x}La_x)Pr_{0.002}InGe_2O_7$ (x = 0–0.2) phosphor calculated using Eq. (1). The η values are all positive, indicating that the lattice environment

Table 1
Lattice parameters and structure for various compositions of $(Y_{0.998-x}La_x)Pr_{0.002}InGe_2O_7$ system.

La content (x)	Lattice parameters			Structure
	a (Å)	b (Å)	c (Å)	
x = 0	6.8296	8.8853	4.9133	Monoclinic
x = 0.03	6.8346	8.8859	4.9139	Monoclinic
x = 0.05	6.8449	8.8915	4.9358	Monoclinic
x = 0.1	6.9138	8.9125	4.9468	Monoclinic
x = 0.2	6.9365	8.9568	4.9687	Monoclinic

Table 2
Strain and grain size of $(Y_{0.998-x}La_x)Pr_{0.002}InGe_2O_7$ system calculated using the Williamson–Hall equation.

La content (x)	η (strain)	d (nm)
x = 0	4.5×10^{-1}	44.95
x = 0.03	1.8×10^{-1}	46.21
x = 0.05	1.6×10^{-1}	50.55
x = 0.1	1.1×10^{-1}	52.18
x = 0.2	4.1×10^{-1}	47.58

experiences tensile strain, which is due to the competition of expansion and shrinkage between the thermal and cooling processes during the heat treatment for phosphor synthesis. η increases and then decreases when the La^{3+} ion content is increased. A η_{max} value of compressive strain (minimum tensile strain) of $x = 0.1$ exists, which has the largest d value (grain size) of 52.18 nm for phosphors. When the La^{3+} ion content is 20 mol%, the internal tensile strain increases and the grain size of phosphors decreases. It is suggested that the secondary phase is produced at grain boundaries and inhibits grain growth.[15] In addition, a material with a nanoscale grain size will have a wide variety of uses, including energy storage, lighting technology, and so on. For nanoscale phosphors, the nanosize particles result in a confinement effect and a large surface area, making them suitable for PL activities with high emission intensities, narrowband emission for high color gamut, and applications requiring high thermal stability.

Figure 2 shows FE-SEM images of the $Y_{0.998}Pr_{0.002}InGe_2O_7$ phosphor doped with various La^{3+} ion contents and calcined at 1200 °C for 10 h in air. These images indicate that the particles are irregular and aggregated. As the La^{3+} ion content increased, the particles seemed to grow and the largest particle size was obtained at 10 mol%. This is consistent with the results shown in Table 2, which indicate that the La^{3+} ion content does not affect the surface morphology, but it affects the grain sizes of the phosphor powders doped with various La^{3+} ion contents. The surface morphology of particles will affect the subsequent optical property performance of phosphors, because to achieve excellent emission efficiency, the phosphor particles should be homogeneous and smooth with a high degree of crystallization, that is, without any aggregates or agglomerates.

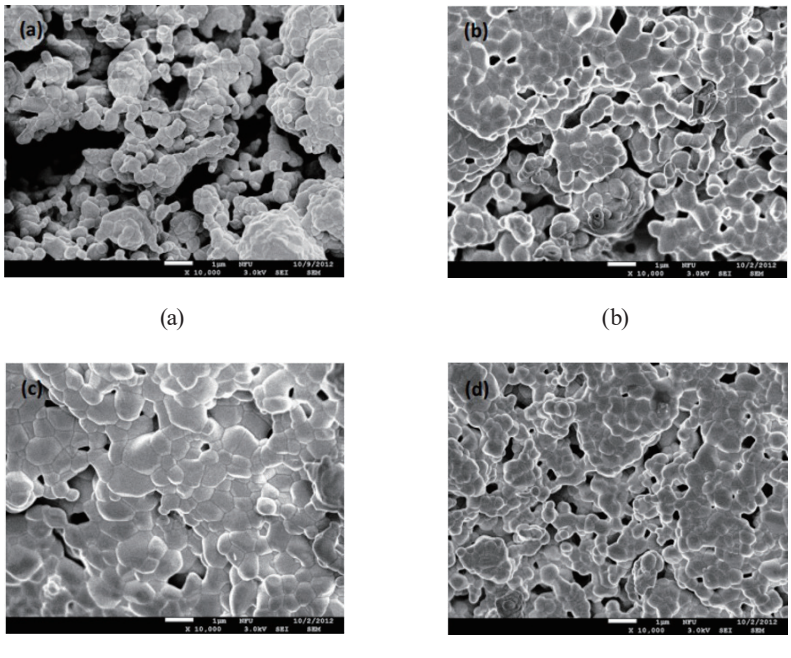

Fig. 2. FE-SEM images of $Y_{0.998}Pr_{0.002}InGe_2O_7$ phosphor doped with various La^{3+} ion contents of (a) 0, (b) 5, (c) 10, and (d) 20 mol%, and calcined at 1200 °C for 10 h.

The excitation spectra of the $Y_{0.998}Pr_{0.002}InGe_2O_7$ phosphor doped with various La^{3+} ion contents and calcined at 1200 °C for 10 h in air are shown in Fig. 3. The signal is detected at 604 nm. In the excitation spectra, a board band is observed in the UV range from 200 to 280 nm corresponding to the charge transfer (CT) between the In^{3+} and O^{2-} ions of the InO_6 anionic group in the host lattice. For the In^{3+} ion, a strong absorption peak is shown in the ultraviolet region because of a d^{10} electron configuration.[16,17] In addition, a shoulder-like absorption band appears from 290 to 450 nm attributed to the oxygen-deficient center of the GeO_4^{4-} anion group.[18] For the oxide-based phosphor, a few oxygen ions will be lost during the high-temperature calcination, and the O^{2-} ions absorbed on the $YInGe_2O_7$ grain surfaces during cooling may give a response of the GeO_4^{4-} group formed. At the same time, vacancies form in the crystalline surface layers because oxygen ions move from the surface layers to the intersite positions. Many weak absorption peaks are observed in the range between 425 and 525 nm, which corresponds to the 4f–4f transition of the Pr^{3+} ion for the $^3H_4 \rightarrow {}^3P_{0,1,2}$ and $^3H_4 \rightarrow {}^1I_6$ radiations.[19]

The emission spectra of the $Y_{0.998}Pr_{0.002}InGe_2O_7$ phosphor doped with various La^{3+} ion contents under 263 nm wavelength excitation are shown in Fig. 4. The broad emission band from 350 to 480 nm is due to the CT process from O^{2-} to In^{3+} within the InO_6 octahedra, which is caused by a recombining process for an electric hole in the ground state and an excited electron in the lowest excitation state. As the La^{3+} ion content increases, the CT emission intensity decreases, and a minimum value exists for 10 mol% La^{3+} ion doping. In addition, emission bands from 475 to 675 nm are related to the 4f–4f transitions of the Pr^{3+} ion corresponding to the $^3P_0 \rightarrow {}^3H_{4,5,6}$ and $^1D_2 \rightarrow {}^3H_4$ radiations. Furthermore, the PL properties of the $Y_{0.998}Pr_{0.002}InGe_2O_7$ phosphor doped with various La^{3+} contents under various internal strains were investigated (discussed in the previous section), and the emission intensity of the 4f–4f $^1D_2 \rightarrow {}^3H_4$ transition of the Pr^{3+} ion can be increased to increase the compressive strain. At a Pr^{3+} ion content of 10

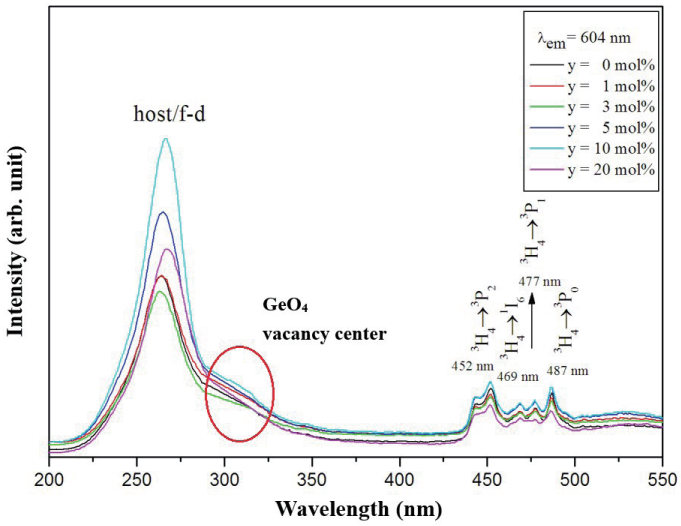

Fig. 3. (Color online) Excitation spectra of $Y_{0.998}Pr_{0.002}InGe_2O_7$ phosphor doped with various La^{3+} ion contents and calcined at 1200 °C for 10 h.

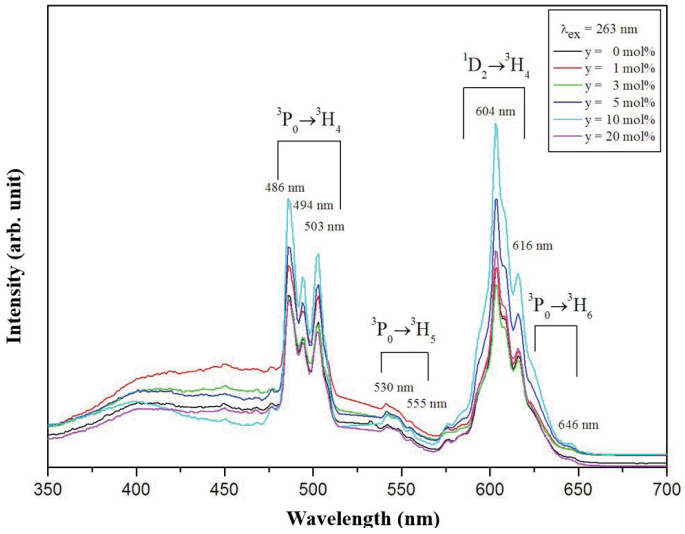

Fig. 4. (Color online) Emission spectra of $Y_{0.998}Pr_{0.002}InGe_2O_7$ phosphor doped with various La^{3+} ion contents under 263 nm wavelength excitation.

mol%, the phosphor exhibits the highest $^1D_2 \rightarrow {}^3H_4$ transition intensity, which is about 60% higher than that of the $Y_{0.998}Pr_{0.002}InGe_2O_7$ phosphor.

The emission behavior of the $Y_{0.998}Pr_{0.002}InGe_2O_7$ phosphor is related to the energy transmission between the f and d energy states of the Pr^{3+} ion. The d energy state is easily split by the crystal field of the host lattice. The strength of the crystal field depends on the lattice symmetry, covalence, electric charge of the ligands, and bond length.[20] These may be represented by the following formula:[21]

$$Dq = \frac{1}{6} Ze^2 \frac{r^4}{R^5}, \tag{2}$$

where Dq is the strength of energy state splitting, Z and e represent the electrical charges of the anion and electron, respectively, r represents the radius of the d wave function, and R is the bond length.

As shown in the results obtained using Eq. (2), Dq will increase when the bond length between the Pr^{3+} ion and the O^{2-} ion decreases. From the emission behavior shown in Fig. 4, the $^1D_2 \rightarrow {}^3H_4$ radiation intensity is higher than that of the $^3P_0 \rightarrow {}^3H_4$ transition. This is because the Y^{3+} ion (0.9Å) was substituted by the La^{3+} ion (1.032 Å), which causes a decrease in bond length between Pr and O and increases in lattice parameters. The smaller Pr–O bond length leads to a higher crystal field strength and enhances the overlap between the 5d wave function of the Pr^{3+} ion and the O^{2-} coordination wave function, which increases the strength of $4f^15d^1$ energy state splitting and induces shifting to a lower energy state.[22] Therefore, a higher emission intensity of the $^1D_2 \rightarrow {}^3H_4$ electron transition was observed. The Pr–O bond lengths in La^{3+} ion-free and La^{3+} ion-doped $Y_{0.998}Pr_{0.002}InGe_2O_7$ crystal structures are illustrated in Fig. 5.

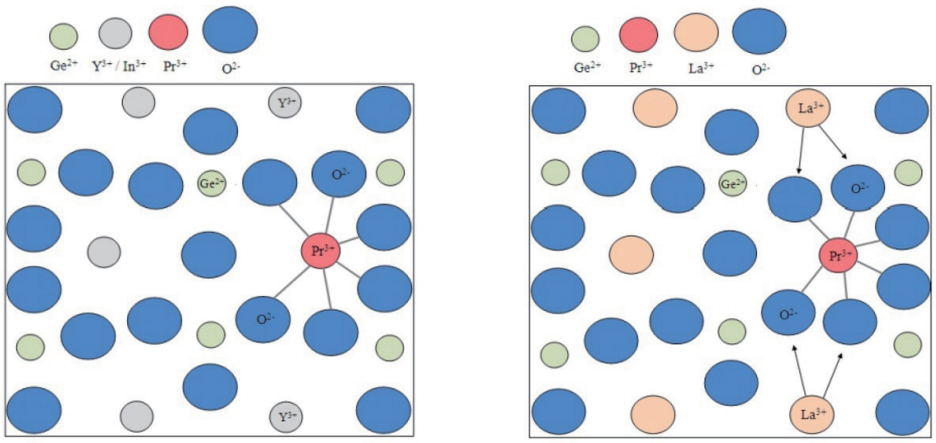

(a) (b)

Fig. 5. (Color online) Illustration of Pr–O bond lengths in (a) $Y_{0.998}Pr_{0.002}InGe_2O_7$ and (b) $Y_{0.898}La_{0.1}Pr_{0.002}InGe_2O_7$ crystal structures.

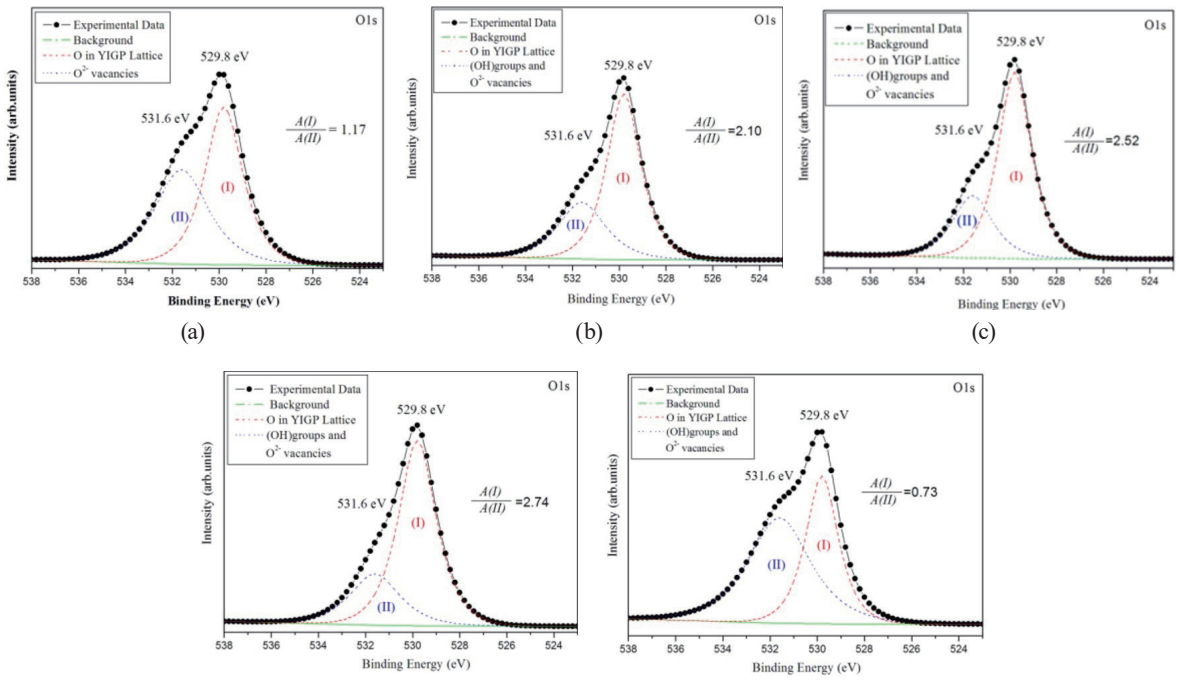

(a) (b) (c)

(d) (e)

Fig. 6. (Color online) XPS of O1s level of $Y_{0.998}Pr_{0.002}InGe_2O_7$ phosphor doped with various La^{3+} ion contents and calcined at 1200 °C for 10 h: (a) 0, (b) 3, (c) 5, (d) 10, and (e) 20 mol%.

The corresponding curve fitting of the O1s level of the $Y_{0.998}Pr_{0.002}InGe_2O_7$ phosphor doped with various La^{3+} ion contents is shown in Fig. 6. In Fig. 6, the fitting is resolved by two peaks, where the red dashed line of curve I centered at the binding energy of 529.8 eV can be ascribed to the oxygen ion in the $Y_{0.998}Pr_{0.002}InGe_2O_7$ (YIGP) lattice and the blue dashed line of curve II centered at the binding energy of 531.6 eV results in oxygen vacancies.[23] The integration area

ratio of the O1s (I) and O1s (II) peaks increases and then decreases with increasing La^{3+} ion content. The maximum area ratio is 2.74 when the La^{3+} ion content is 10 mol%. According to the study, at a temperature higher than 1000 °C, the electrically neutral oxygen located on the regular oxygen lattice may be excited into the conduction band by emitting two electrons, leaving behind oxygen vacancies with a twofold ionized positivity, $V_{\ddot{O}}$, in the lattice, and it may be represented by the following reaction:[24]

$$O_O^x \leftrightarrow \frac{1}{2} + V_{\ddot{O}} + 2e'. \tag{3}$$

The results indicate that when the compressive strain increases in phosphor host lattices, the oxygen vacancy formation energy increases, reducing the concentration of oxygen vacancies and increasing the emission intensity.[25] On the basis of the results mentioned above, η is minimum, whereas the emission intensity is highest when the La^{3+} ion content is 10 mol%. A small ion (Y^{3+}) replaced by a large ion (La^{3+}) in the $Y_{0.998}Pr_{0.002}InGe_2O_7$ phosphor will introduce a compressive strain to inhibit oxygen formation and enhance PL.

Figure 7 shows the CIE color coordinate diagram of the $Y_{0.998}Pr_{0.002}InGe_2O_7$ phosphor doped with various La^{3+} ion contents under 263 nm wavelength excitation. With increasing La^{3+} ion content, there are some variations in color coordinates, but they are all in the white light region. The color tones of the $Y_{0.998}Pr_{0.002}InGe_2O_7$ phosphor emission can be modulated by determining the La^{3+} ion content.

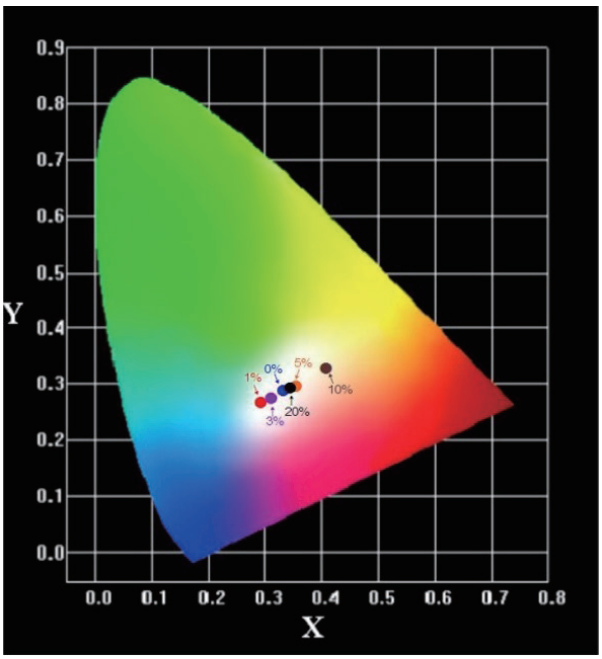

Fig. 7. (Color online) CIE color coordinate diagram of $Y_{0.998}Pr_{0.002}InGe_2O_7$ phosphor doped with various La^{3+} ion contents under 263 nm wavelength excitation.

4. Conclusions

Doping the La^{3+} ion at various concentrations on a single-phased white light-emitting phosphor, $Y_{0.998}Pr_{0.002}InGe_2O_7$, was carried out by the vibration mill method, and a solid-state reaction was performed with calcination at 1200 °C for 10 h. The doping of an appropriate La^{3+} ion concentration distorted the host lattice and an increase in compressive strain was induced to reduce the oxygen vacancy concentration, which improved the PL properties of the $Y_{0.998}Pr_{0.002}InGe_2O_7$ phosphor. The Pr^{3+} ion 4f–4f transition intensities and emission color tone of La^{3+} ion-doped $Y_{0.998}Pr_{0.002}InGe_2O_7$ phosphors can be modulated by adjusting the La^{3+} ion concentration. Most of all, a phosphor maintains its original structure and single-phased white light emission characteristics do not change with La^{3+} ion doping. La^{3+} ion doping not only can improve the PL properties of the $Y_{0.998}Pr_{0.002}InGe_2O_7$ single-phased white light-emitting phosphor but also can be applied to oxygen gas sensors.

Acknowledgments

The authors would like to thank the National Science and Technology Council of Taiwan for financially supporting this research under Grant No. NSTC 109-2622-E-150-006-CC3.

References

1 Y. Shimizu, K. Sakano, Y. Noguchi, and T. Moriguchi: US Patent No. 5998925 (1998).
2 L. X. Yi, Y. B. Hou, H. Zhao, D. W. He, Z. Xu, Y. S. Wang, and X. R. Xu: Displays **21** (2000) 147. https://doi.org/10.1016/S0141-9382(00)00046-9
3 B. S. Tsai, Y. H. Chang, and Y. C. Chen: J. Mater. Res. **19** (2004) 1504. https://doi.org/10.1557/JMR.2004.020
4 T. Minami: Solid State Electron. **47** (2003) 2237. https://doi.org/10.1016/S1002-0721(07)60531-6
5 W. Wang, C. G. Jiang, M. R. Shen, L. Fang, F. G. Zheng, X. L. Wu, and J. C. Shen: Appl. Phys. Lett. **94** (2009) 081904. https://doi.org/10.1063/1.3089814
6 Y. S. Chang, F. M. Huang, H. L. Chen, and Y. Y. Tsai: J. Phys. Chem. Solids **72** (2011) 1117. https://doi.org/10.1016/j.jpcs.2011.06.008
7 Y. S. Chang, F. M. Huang, Y. Y. Tsai, and L. G. Teoh: J. Lumin. **129** (2009) 1181. https://doi.org/10.1016/j.jlumin.2009.05.020
8 Y. S. Chang, H. R. Shih, M. T. Tsai, K. T. Liu, and L. G. Teoh, J. Lumin. **157** (2015) 98. https://doi.org/10.1016/j.jlumin.2014.07.024
9 Y. Y. Tsai, M. T. Tsai, H. T. Lin, and Y. S. Chang: J. Alloy. Compds. **581** (2013) 35. https://doi.org/10.1016/j.jallcom.2013.05.217
10 L. G. Teoh, M. T. Tsai, Y. C. Chang, and Y. S. Chang: Ceram. Inter. **44** (2018) 2656. https://doi.org/10.1016/j.ceramint.2017.10.163
11 C. S. Chu and T. H. Lin: Sens. Actuators, B **210** (2015) 302. https://doi.org/10.1016/j.snb.2014.12.133
12 P. Bountinaud, R. Mahiou, E. Cavalli, and M. Bettinelli: J. Lumin. **122–123** (2007) 430. https://doi.org/10.1016/j.jlumin.2006.01.198
13 E. A. Juarez-Arellano, L. Bucio, J. L. Ruvalcaba, R. Moreno-Tovar, J. F. Garcia-Robledo, and E. Orozco: Z. Kristallogr. **217** (2002) 201. https://doi.org/10.1524/zkri.217.5.201.20636
14 G. K. Williamson and W. H. Hall: Acta. Metall. **1** (1953) 22. https://doi.org/10.1016/0001-6160(53)90006-6
15 D. Hennings, A. Schnell, and G. Simon: J. Am. Ceram. Soc. **65** (1982) 539. https://doi.org/10.1111/j.1151-2916.1982.tb10778.x
16 G. Blasse, G. J. Dirksen, N. Kimizuka, and T. Mohri: Mat. Res. Bull. **21** (1986) 1057. https://doi.org/10.1016/0025-5408(86)90221-7
17 G. Blasse: Chem. Phys. Lett. **175** (1990) 237. https://doi.org/10.1016/0009-2614(90)85549-R

18 N. Kristianpoller, A. shmilevich, D. Weiss, R. Chen, and N. Khaidukov: Rad. Meas. **33** (2001) 637. https://doi.org/10.1016/S1350-4487(01)00074-9
19 P. Boutinaud, E. Pinel, M. Duboism, A. P. Vink, and R. Mahiou: J. Lumin. **111** (2005) 69. https://doi.org/10.1016/j.jlumin.2004.06.006
20 J. S. Kim, J. Y. Kang, P. E. Jeon, J. C. Choi, H. L. Park, and T. W. Kim: Jpn. J. Appl. Phys. **43** (2004) 989. https://doi.org/10.1143/JJAP.43.989
21 P. D. Rack and P. H. Holloway: Mater. Sci. Eng., R **21** (1998) 171. https://doi.org/10.1016/S0927-796X(97)00010-7
22 C. de Mello Donegá, A. Meijerink, and G. Blass: J. Phys. Chem. Solids **56** (1995) 673. https://doi.org/10.1016/0022-3697(94)00183-9
23 Q. Zou, H. Ruda, B. G. Yacobi, and M. Farrell: Thin Solid Film **402** (2002) 65. https://doi.org/10.1016/S0040-6090(01)01708-4
24 R. Moos and K. H. Hardtl: J. Am. Ceram. Soc. **80** (1997) 2549. https://doi.org/10.1111/j.1151-2916.1997.tb03157.x
25 J. D. Sayre, K. T. Delaney, and N. A. Spaldin: Preprint arXiv:1202.1431 (2012). https://doi.org/10.48550/arXiv.1202.1431

About the Authors

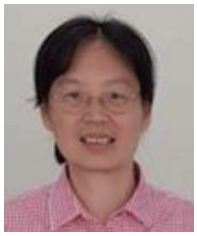

Lay Gaik Teoh is a professor in the Department of Mechanical Engineering of National Pingtung University of Science and Technology, Pingtung, Taiwan. Her research interests include phosphor materials, dielectric materials, gas sensors, and nanomaterials. (n5888107@gmail.com)

Sean Wu received his B.S. degree in electrical engineering from Chung Yuan Christian University in Taiwan in 1993, and his M.S. and Ph.D. degrees in electrical engineering from National Cheng Kung University in 1995 and 2001, respectively. He joined the Department of Electronics Engineering and Computer Science of Tung Fang Design University and became a professor in 2010. Since 2020, he has been a professor at Lunghwa University of Science and Technology. His research interests are in the fabrication of piezoelectric thin films, the design of acoustic wave devices, and substrate materials for SAW and FBAR devices. (wusean.tw@gmail.com)

Hao-Long Chen received his B.S. degree from National Taiwan Ocean University, Taiwan, in 1991, his M.S. degree from National Taiwan University of Science and Technology, Taiwan, in 1994, and his Ph.D. degree from National Cheng Kung University, Taiwan, in 2005. His research interests are in phosphor materials, sensor materials, energy materials, and nanomaterials. (hlchern@ms18.hinet.net)

Kuan-Ting Liu received his B.S. degree from the Department of Electrical, Electronics and Computer Engineering, Waseda University, Tokyo, Japan, in 1998, his M. S. degree in electrical engineering from Waseda University, Tokyo, Japan, in 2000, and his Ph. D. degree from the Institute of Microelectronics and Department of Electrical Engineering, National Cheng Kung University, Tainan, Taiwan, in 2005. His research interests include thin-film processing and optoelectronic devices. (k0421@gcloud.csu.edu.tw)

Yee-Shin Chang received his M.S. and Ph.D. degrees from National Cheng Kung University, Taiwan, in 2000 and 2004, respectively. From 2004 to 2006, he was a principal engineer in United Microelectronics Corporation (UMC) in Taiwan. From 2006 to 2009, he was an assistant professor at National Formosa University, Taiwan. Since 2012, he has been a professor at National Formosa University. His research interests are in phosphor powder synthesis, dielectric ceramics, and electro-optic ceramics. (yeeshin@nfu.edu.tw)